



Fàbrega, J. M., Moreolo, M. S., Mayoral, A., Vilalta, R., Casellas, R., Muñoz, R., Yoshida, Y., Kitayama, K., Kai, Y., Nishihara, M., Okabe, R., Tanaka, T., Takahara, T., Rasmussen, J. C., Yoshikane, N., Cao, X., Tsuritani, T., Morita, I., Habel, K., ... Wada, N. (2017). Demonstration of Adaptive SDN Orchestration: A Real-time Congestion-aware Services Provisioning over OFDM-based 400G OPS and Flexi-WDM OCS. *Journal of Lightwave Technology*, 35(3), 506-512. <https://doi.org/10.1109/JLT.2017.2655418>

Peer reviewed version

Link to published version (if available):
[10.1109/JLT.2017.2655418](https://doi.org/10.1109/JLT.2017.2655418)

[Link to publication record in Explore Bristol Research](#)
PDF-document

This is the author accepted manuscript (AAM). The final published version (version of record) is available online via IEEE at <http://ieeexplore.ieee.org/document/7822967>. Please refer to any applicable terms of use of the publisher.

University of Bristol - Explore Bristol Research

General rights

This document is made available in accordance with publisher policies. Please cite only the published version using the reference above. Full terms of use are available:
<http://www.bristol.ac.uk/red/research-policy/pure/user-guides/ebr-terms/>

Demonstration of Adaptive SDN Orchestration: A Real-time Congestion-aware Services Provisioning over OFDM-based 400G OPS and Flexi-WDM OCS

J. M. Fàbrega, M. Svaluto Moreolo, A. Mayoral, R. Vilalta, R. Casellas, R. Martínez, R. Muñoz, Y. Yoshida, K. Kitayama, Y. Kai, M. Nishihara, R. Okabe, T. Tanaka, T. Takahara, J. C. Rasmussen, N. Yoshikane, X. Cao, T. Tsuritani, I. Morita, K. Habel, R. Freund, V. López, A. Aguado, S. Yan, D. Simeonidou, T. Szyrkowiec, A. Autenrieth, M. Shiraiwa, Y. Awaji, N. Wada

(Post-Deadline)

Manuscript received June 1, 2016; revised MMMM DD, YYYY; accepted MMMM DD, 2016. Date of publication MMMM DD, YYYY; date of current version MMMM DD, YYYY. This work was supported by FP7 EU-Japan Project STRAUSS (GA 608528, 2014–2016), and the MINECO project TEC2015-69256-R (DESTELLO). This paper was presented in part as a post-deadline paper at IEEE/OSA OFC [1].

J. M. Fàbrega, M. Svaluto Moreolo, A. Mayoral, R. Vilalta, R. Casellas, R. Martínez and R. Muñoz are with the Centre Tecnològic de Telecomunicacions de Catalunya, 08860 Barcelona, Spain (e-mail: jmfabrega@cttc.es, msvaluto@cttc.es, amayoral@cttc.es, rvilalta@cttc.es; rcasellas@cttc.es; rmartinez@cttc.es; rmunoz@cttc.es)

Y. Yoshida, was with the Graduate School of Engineering, Osaka University, Suita, Osaka 565-0871, Osaka University, Osaka, Japan. He is now with the NICT, Koganei, Japan (email: yuki@nict.go.jp).

K. Kitayama was with the Graduate School of Engineering, Osaka University, Suita, Osaka 565-0871, Osaka University, Osaka, Japan. He is now with the Graduate School for the Creation of New Photonics Industries, Hamamatsu, Shizuoka 431-1202. (e-mail: kitayama@gpi.ac.jp).

Y. Kai, M. Nishihara, R. Okabe, T. Tanaka, T. Takahara and J. C. Rasmussen are with Fujitsu Labs Ltd., Kawasaki, Kanagawa 211-8588, Japan (e-mail: kai@jp.fujitsu.com; mnishi@jp.fujitsu.com; okabe.ryou@jp.fujitsu.com; ttohsiki@jp.fujitsu.com; tomoo.takahara@jp.fujitsu.com; jens.rasmussen@jp.fujitsu.com).

N. Yoshikane, X. Cao, T. Tsuritani, and I. Morita are with KDDI R&D Labs. Saitama, Japan. (e-mail: yoshikane@kddilabs.jp; xi-cao@kddilabs.jp; tsuri@kddilabs.jp; morita@kddilabs.jp).

K. Habel and R. Freund are with the Fraunhofer HHI, Berlin 10587, Germany (e-mail: kai.habel@hhi.fraunhofer.de; Ronald.Freund@hhi.fraunhofer.de).

V. López is with Telefónica I+D, 28080, Madrid, Spain. (e-mail: victor.lopezalvarez@telefonica.com).

A. Aguado, S. Yan and D. Simeonidou are with the High-Performance Networks Group, University of Bristol, Bristol, BS8 1TH, U.K. University of Bristol, Bristol, United Kingdom. (e-mail: a.aguado@bristol.ac.uk, Shuangyi.Yan@bristol.ac.uk, dimitra.simeonidou@bristol.ac.uk)

T. Szyrkowiec and A. Autenrieth are with ADVA Optical Networking, Munich 82152, Germany (e-mail: tszyrkowiec@advaoptical.com, autenrieth@advaoptical.com).

M. Shiraiwa, Y. Awaji and N. Wada are with National Institute of Information and Communications Technology (NICT), Tokyo 184-8795, Japan (e-mail: shiraiwa@nict.go.jp; yossy@nict.go.jp; wada@nict.go.jp)

Color versions of one or more of the figures in this paper are available online at <http://ieeexplore.ieee.org>

Digital Object Identifier XXXXXXXXXXXXXXXXXXXX

Abstract— In this work, we experimentally demonstrate highly flexible and intelligent inter-domain coordinated actions based on adaptive software-defined networking (SDN) orchestration. An advanced multi-domain multi-technology testbed is implemented, which consists of a 400-Gb/s variable-capacity optical packet switching domain and a Tb/s-class flexi-grid wavelength division multiplexed optical circuit switching domain. The SDN-controllable transponders and the extended transport applications programming interface (API) enable the congestion-aware provisioning of end-to-end real-time services. At the data plane level, different transponders based on orthogonal frequency division multiplexing (OFDM) are employed for inter/intra-domain links in order to adaptively provision services with fine granularity. For adaptation, SDN-capable domain-specific optical performance monitors are also introduced. In the control plane, the applications based network operations (ABNO) architecture has been extended and addressed as an adaptive SDN orchestrator.

Index Terms— Multicarrier modulation, discrete multi-tone, OFDM, flexi-grid networks, optical packet switching, software-defined networking, sliceable bandwidth variable transceiver (S-BVT).

I. INTRODUCTION

SOFTWARE-DEFINED networking (SDN) orchestration has been proposed and demonstrated as a feasible solution to efficiently manage end-to-end services in network scenarios including multiple domains, technologies, and tenants [1][2][3][4]. Key enablers are i) the control orchestration protocol (COP) [5] for a transport applications programming interface (API) to allow interworking of heterogeneous control plane paradigms (e.g., OpenFlow, GMPLS/PCE) and ii) the domain-specific sliceable bandwidth/bitrate variable transponders (S-BVTs) to provide bandwidth adaptive end-to-end services [2][6][7].

In this work, we experimentally demonstrate highly flexible and intelligent inter-domain coordinated actions based on the

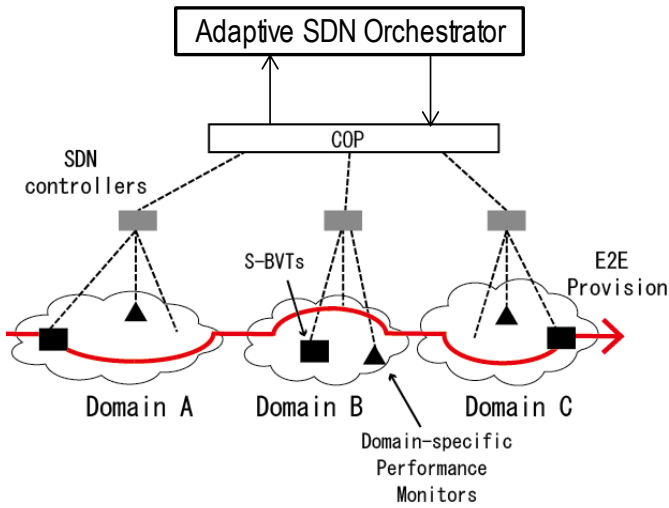


Fig. 1. Adaptive SDN orchestration concept for end-to-end (E2E) connection provisioning.

software-defined networking adaptive orchestration of different network domains. As depicted in Fig. 1, the key adaptive element is the SDN orchestrator. There, real-time network monitoring information is processed to validate and provide optimal selection of network resources for satisfying the new end-to-end service demands and dynamically re-optimize those service demands based on current network state. Thus, domain-specific performance monitoring plays a key role in order to allow the pursued adaptive orchestration. Fig. 1 also shows other key elements for the proposed adaptive SDN orchestration, including the S-BVTs and the domain-specific SDN controllers. The latter are in charge of each network domain, which can be of different nature, and are interfaced with the adaptive SDN orchestrator by means of the COP. This last provides the suitable framework for the end-to-end connection provisioning by interworking of different heterogeneous domains [3].

In order to demonstrate the adaptive SDN orchestration concept, an advanced multi-domain/technology testbed is implemented. It consists of a 400-Gb/s variable-capacity optical packet switching (OPS) domain and a flexi-grid wavelength division multiplexed (WDM) optical circuit switching (OCS) domain, featuring beyond 1-Tb/s capacity, each controlled by the corresponding individual SDN controllers. In the data plane, different S-BVTs, based on discrete multi-tone (DMT) and orthogonal frequency division multiplexing (OFDM), are employed for inter/intra-domain links enabling adaptive and fine granular end-to-end service provisioning. SDN-capable domain-specific optical performance monitors, including high resolution optical channel monitor, are also introduced. In the control plane, the applications based network operations (ABNO) architecture [2][8] has been extended and addressed as an adaptive SDN orchestrator. As a use case, we demonstrate a real-time congestion-aware provisioning of end-to-end services including an inter-domain high definition (HD) video streaming. The orchestrator detects traffic congestion of specific flows, allowing congestion control (e.g. via DMT

rate-adaptation for packet compression) in the OPS domain, and improves the quality of service (QoS) of the end-to-end services in a self-healing manner.

The paper is structured as follows. In section II the actual testbed implementation details are provided. Afterwards, section III describes the analyzed use case, which is a congestion-aware inter-domain service provisioning in real time. Section IV deals with the experiment results. Finally, conclusions are drawn in section V.

II. TESTBED IMPLEMENTATION

The data plane of our testbed was implemented at NICT premises in Sendai, Japan. The data plane included two network domains: a 400G-class DMT-based OPS network and a Tb/s-class flexi-WDM OCS network. Each domain was controlled by an individual custom SDN controller located at KDDI Labs premises in Saitama, Japan, and connected through JGN-X [9]. Both domains were orchestrated by an adaptive SDN orchestrator deployed at CTTC premises in Castelldefels (Barcelona), Spain, through a virtual private network (VPN) connection.

In the data plane, the OPS domain consisted of 4 OPS nodes (A-D) shown in Fig. 2 (center). A 400G (4 wavelengths running at 100G) DMT and a 100G-OOK (10 wavelengths running at 10G) were employed as optical payload formats. As shown in Fig. 1a, the nodes A-C were based on 4×4 switches (SWs) based on semiconductor optical amplifiers [10], while node D employed a 4×4 PLZT SW for the transparent switching of the DMT packets. The 100G packet transponders at nodes A-B were real-time and had a 10G Ethernet client signal interface. A semi-real-time DMT packet transmitter was implemented at node C and the receiver was at the output of node D.

The DMT signal was generated by a field programmable gate array (FPGA) and converted to an analog signal by a 64 GS/s, 8 bits digital-to-analog converter (DAC). The laser wavelengths were modulated by Mach-Zehnder modulators (MZM) and multiplexed. The transmitted DMT packet was received by a photodetector (PD) through the demultiplexer (DEMUX). The received signal was converted to digital by a 64 GS/s, 8 bits analog-to-digital converter (ADC) and subsequently demodulated by the FPGA. The subcarrier number and the cyclic prefix of the DMT signal were 1024 and 16, respectively.

Most of the network entities in the domain were SDN-controllable. Particularly, the DMT transponder could be programmed, i.e. had the capability to adapt the payload format based on policy (e.g., full-rate, half-rate, energy-saving etc.) given by the SDN controller. This capability plays an important role in the operation of optical networks, by supporting the on-demand configuration of programmable network functions, such as rate, bandwidth, path adaptation, and slice-ability, enabling to handle variable granularity (including the sub-wavelength level). In particular, spectral manipulation at the subcarrier level is possible for optimizing the transmission performance and the transceiver capacity, according to the network priority to meet the traffic demand, the available bandwidth, the path/channel and energy efficiency requirements. So, we approached a policy-based control in the

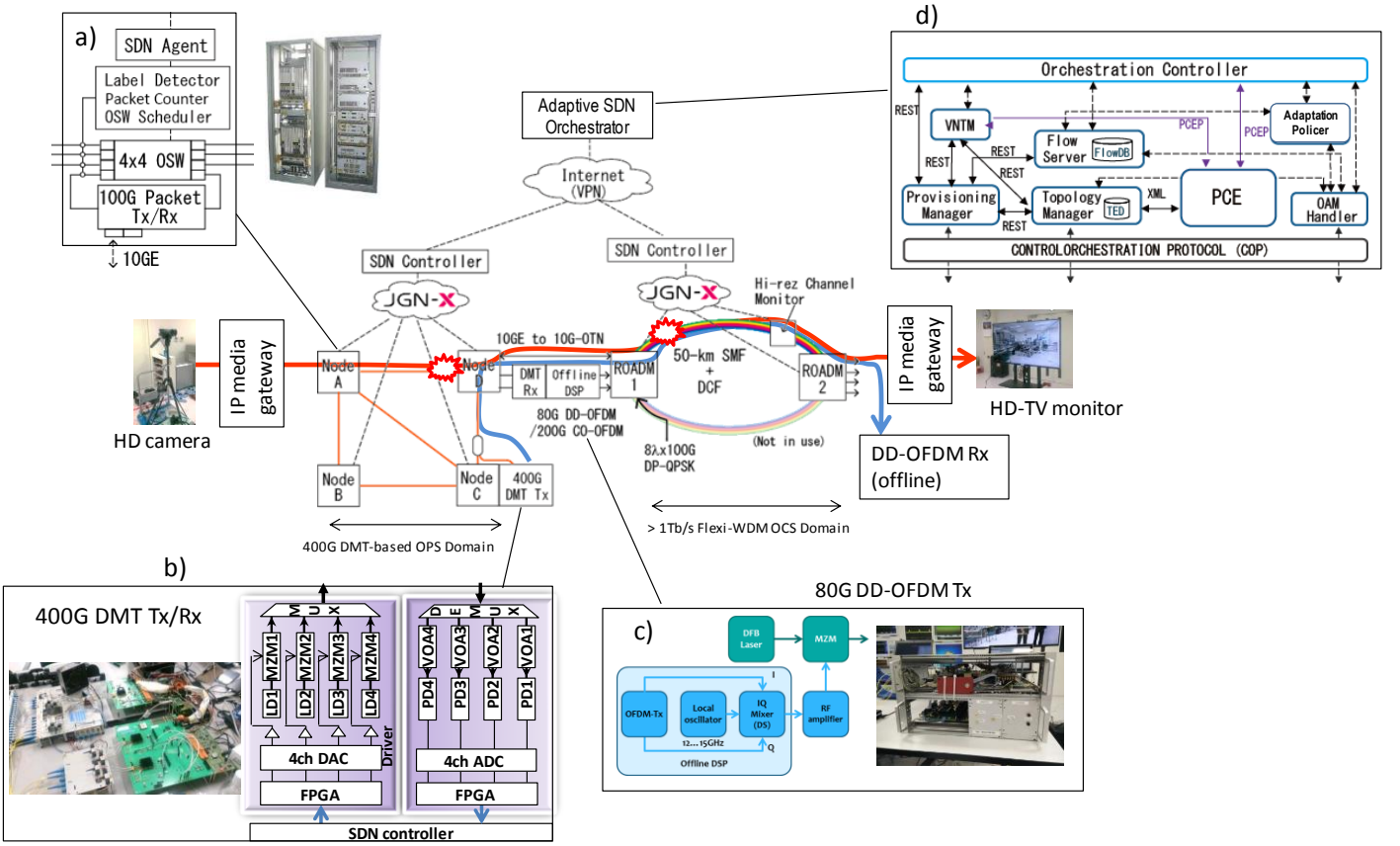


Fig. 2. Testbed implementation. (a) Scheme of the OPS nodes. Internal architecture of (b) the 400G DMT transponder and (c) the 80G DD-OFDM transponder. (d) Scheme of the adaptive SDN orchestrator.

DMT transponders in view of its integration in an SDN based control plane. Therefore, in case of capacity priority, the DMT transponder enabled flexible rate/distance by adaptively assigning the suitable number of bits per symbol per subcarrier.

As performance monitors to enable adaptive orchestration, optical packet counters (OPCs) were implemented at each node, which reported on link congestion to the SDN controller.

The OCS domain was a 50-km diameter ring network with 2 flexi-grid reconfigurable optical add/drop multiplexers (ROADMs 1-2) based on 1×4 programmable wavelength selective switches (WSSs). At ROADM 1, a single S-BVT was deployed as the OPS-to-OCS interface, featuring 3 different slices: a 200G (48Gbaud, 32QAM) single-polarization coherent optical (CO) OFDM, an 80G direct detection (DD) OFDM, and a 10G-OTN (i.e. OTU2e) sub-transponder. Both OFDM sub-transponders were implemented with offline digital signal processing (DSP), while the 10G-OTN was carrying real-time data.

The DD-OFDM signal, carrying 1024 subcarriers was generated as follows (See Fig. 2c). The Inphase (I) and Quadrature (Q) components were digitally upconverted to an intermediate local oscillator (LO) frequency of 15 GHz. The electrical spectrum occupied the range within 3 GHz and 27 GHz. The upconverted OFDM signal was imprinted on a laser source using an intensity Mach-Zehnder modulator (MZM) and transmitted over the link. At the receiver side, the signal was detected using an integrated PIN+TIA module and

digitally post-processed using offline DSP.

The bandwidth of the S-BVT was decided via the SDN controller depending on the reach/purpose of the established connections. For example, DD-OFDM was conceived for coping with metro-access distances. In addition, $8\lambda \times 100G$ dual polarization quadrature phase shift keying (DP-QPSK) channels were implemented to demonstrate flexi-WDM network operation beyond 1-Tb/s. A non-intrusive optical performance monitoring system was deployed at the ROADMs. This domain was heterogeneous, as it included different optical signals, depending on the reach/purpose of the established connections. Thus, the deployed monitoring system was able to scan the whole C-band and automatically extract the different performance parameters, including WDM channel allocation, effective guard-band, signal power and optical signal to noise ratio (OSNR) of each multi-format flexi-WDM channel. The main blocks composing the signal monitor were a 10-MHz-resolution optical spectrum analyzer, a signal processing module, a notification server and a monitoring agent. The spectrum analysis was performed by the signal processing module, which was also in charge of deriving the corresponding performance parameters that fed the monitoring agents. This allowed to suitably configure the different domain network resources, including the parameters of the transponders, according to the signal quality [11].

The SDN orchestrator was based on the ABNO architecture (Fig. 2d) using a COP based on YANG/RESTCONF [12] as a

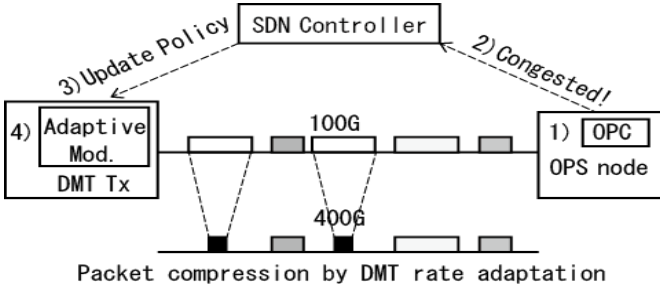


Fig. 3 SDN-enabled OPS congestion control use case: DMT rate-adaptation (a) and the corresponding control log at the SDN agent.

unified interface towards the OCS/OPS SDN controllers. To enable the adaptive orchestration of resources, its ABNO architecture was extended by newly adding an adaptation policer module, which provided updates on the optimization criteria to the orchestrator controller. Such an optimization criteria was based on the network status information received from the control plane through the operation and monitoring (OAM) handler (Fig. 2d). The different monitoring agents send the monitoring data to the corresponding domain controller notification server through websockets. Then, the SDN controller of each domain forwarded the monitoring information to the adaptive SDN orchestrator through the COP CallUpdate/Remove notification messages, using websockets as well.

III. USE CASE CONGESTION-AWARE REAL-TIME INTER-DOMAIN SERVICE PROVISIONING

In this section, we introduce a use case where adaptive SDN orchestration is applied to solve congestion and provide concurrent optimization for both OPS and OCS domains in order to provision end-to-end services.

Fig. 3 shows the SDN-enabled OPS congestion control use case. The OPC in the OPS node monitors the received amount of optical packets. If the monitored packet count reaches a pre-determined threshold (step 1 in Fig. 3), the optical packet counter automatically sends an alarm to the SDN controller in order to notify an occurrence of packet congestion (step 2). When the SDN controller receives the alarm, the SDN controller sends a message (step 3) to a rate-adaptive transmitter (DMT Tx) in order to change the bitrate of a packet flow (step 4), aiming at reducing the packet loss ratio while preserving the transmission capacity [13].

With respect to the OCS domain, Fig. 4 shows a representation of a portion of the spectrum of a flexi-WDM link with a set of already established, channels (A, B, C), being A the channel providing end-to-end connection. Congestion occurs when a new connection request (channel D) demands a specific spectrum slot, which is unavailable (step I). Following a specify-TE policy (i.e., the use of low cost transponders with potentially limited tunability), the adaptive SDN orchestrator triggers a spectrum re-allocation of channels B and C (step II) to fit signal D within the spectrum range specified by request D. Following a maximum spectrum efficiency policy, channel D is allocated with the minimum guard band to channel A. After the connection has been established, the signal monitoring detects

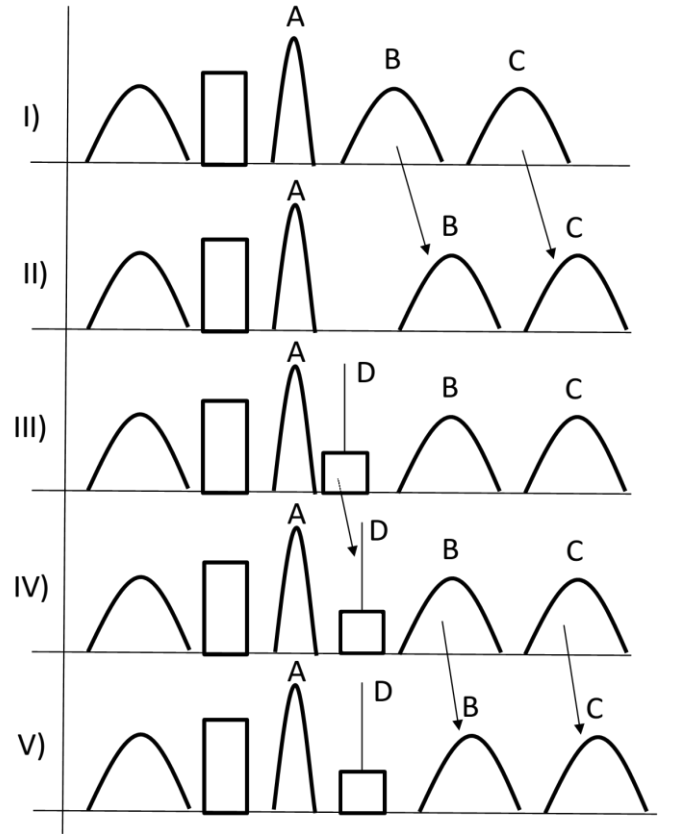


Fig. 4. OCS congestion control use case: spectrum re-allocation and guard-band adjustment.

interference within a portion of the spectrum and notifies the SDN controller. The controller identifies that channel A is affected and notifies the orchestrator. In response, the SDN orchestrator identifies that channel D has caused the interference (since it was the last channel created) and increases the guard band between them by re-allocating channel D accordingly via the SDN controller (step IV). A heuristic algorithm is applied for adaptive resource orchestration: The guard band between channels is gradually incremented until no signal degradation is detected. Such a guard band value is then incorporated to the knowledge base of the SDN orchestrator. Finally, the SDN orchestrator re-allocates channels B and C following a similar procedure (step V in Fig. 4).

IV. EXPERIMENTAL RESULTS

As mentioned in section III real-time congestion-aware provisioning of end-to-end services was demonstrated in the multi-domain testbed. In the demo, two inter-domain flows were generated. One was for the real-time HD video streaming. A full-HD camera with IP-based media gateway was located at node A in the OPS domain, while another gateway and a HD display system were at the ROADM 2 (as shown in Fig. 2). The video traffic was based on 10G Ethernet and converted to a 10G-OTN signal at node D in real-time. Another flow originated from the DMT transmitter at node C. This flow was logically interfaced by the DD-OFDM transmitter at node D and then transferred to the ROADM 2 as well. The effective bit rate of this flow was around 15 Gb/s (packet rate was 17% at

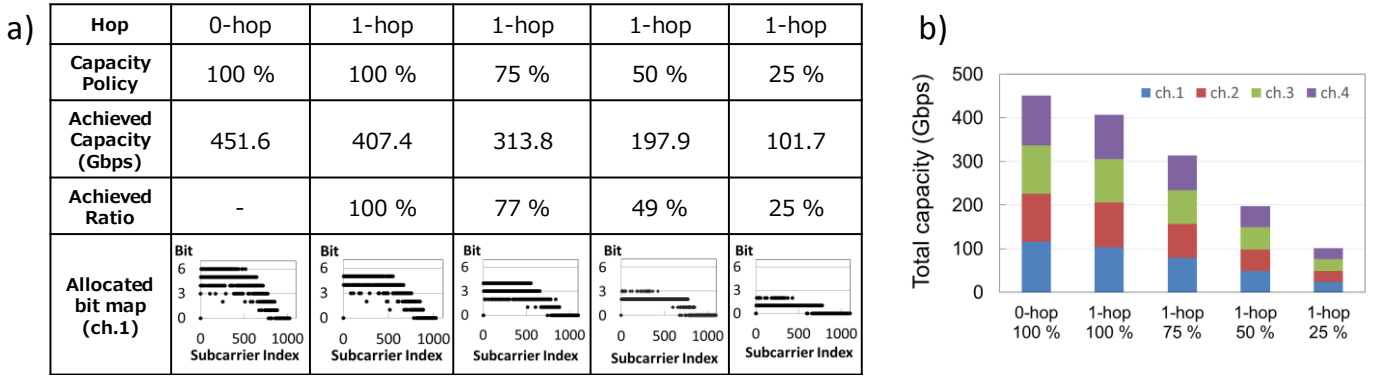


Fig. 5. Achieved bit rate of DMT packets.

100G).

A. OPS domain

In the OPS domain, first, the controller learnt some thresholds for the OPC value to sustain the intra-domain packet loss ratio (PLR) below 1 % in an offline manner. After setting the two flows, the packet counter at node D detected the congestion (1-2 in Fig. 3). To avoid the optical packet contention, the controller decided to change the transmission policy for the DMT flow (3 in Fig. 3). Then, the DMT transmitter compressed the optical packets in the time domain to reduce the link occupancy by the adaptive modulation (4 in Fig. 3). Figs. 5a-b show the characteristics of the semi-real-time DMT transponder with different transmission policies. The total achievable capacity was up to 407.4 Gb/s ($100G \times 4\lambda$) after 1 hop.

When the capacity policy was changed to 75 %, 50 %, and 25 %, achieved ratio of the total capacity of 4-lanes was decreased to 77 %, 49 %, and 25 %, respectively. We could find that the allocated bitmap of the DMT signals was changed corresponding to the target capacity from Fig. 5a. From these results, we demonstrated the policy-based control of the DMT transponder from the SDN controller.

The control log at the agent SDN agent for the proposed SDN-enabled OPS congestion control is shown in Fig. 6. There it can be observed that all the steps regarding congestion control procedure (1-4 in Fig. 3) could be successfully executed within a few seconds.

The control traffic messages are depicted in Fig. 7. Precisely, in Fig. 7a-c we can see how the different domains are properly initialized. When the packet count read from the OPC module of OPS node D reached the pre-defined threshold, indicating traffic congestion as shown (1-2) in Fig. 6, the SDN agent attached to OPS node D detected this packet congestion and sent an alarm message to the SDN controller.

As shown in Fig. 7d, the SDN controller then sent a notification to the adaptive SDN orchestrator to adjust the DMT-based rate adaptive transmitter to decrease the packet occupancy rate and increase the bit rate of signal from 100 Gb/s to 400 Gb/s, so as to alleviate the traffic congestion while preserving the transmission capacity.

B. OCS domain

In the OCS domain, the adaption was needed particularly to

```

134 18:03:18,948: cont_osaka: total 804871 threshold 1000000
135 18:03:23,967: cont_osaka: received cnt (1405601, 0, 0, 0, 0, 0, 0, 0, 0, 0, 0, 0, 0, 0, 0, 0, 0, 0, 0, 0)
1-2) 136 18:03:23,967: cont_osaka: total 1405601 threshold 1000000
137 18:03:23,967: agent: command response nothing
3-4) 138 18:03:23,968: agent: command {"cmd":"/dmtransctrl policy 1", "node":"fujitsu"}
139 18:03:23,968: cont: node fujitsu
140 18:03:23,968: cont: login windows 7 192.168.1.59
141 18:03:26,966: cont: error [Errno 113] No route to host
142 18:03:26,967: agent: command response nothing
143 18:03:26,967: agent: command {"cmd":"/test", "node":"opstx1", "policy":"1"}

```

Fig. 6 Control log at the SDN agent for the proposed SDN-enabled OPS congestion control.

```

Client      C-SDN ORCH HTTP POST /restconf/config/calls/call/0
C-SDN ORCH OPS SDN CTRL HTTP POST /restconf/config/calls/call/00001/
C-SDN ORCH OPS SDN CTRL HTTP POST /restconf/config/calls/call/00002/
Client      C-SDN ORCH HTTP POST /restconf/config/calls/call/A
C-SDN ORCH OPS SDN CTRL HTTP POST /restconf/config/calls/call/00003/
C-SDN ORCH OPS SDN CTRL HTTP POST /restconf/config/calls/call/00004/
C-SDN ORCH OPS SDN CTRL HTTP POST /restconf/config/calls/call/00005/
C-SDN ORCH OPS SDN CTRL HTTP POST /restconf/config/calls/call/00006/
OPS SDN CTRL C-SDN ORCH WebSocket WebSocket Text [FIN]

OPS
  Client      C-SDN ORCH HTTP POST /restconf/config/calls/call/0
  C-SDN ORCH OPS SDN CTRL HTTP POST /restconf/config/calls/call/00007/
  C-SDN ORCH OPS SDN CTRL HTTP POST /restconf/config/calls/call/00008/
  Client      C-SDN ORCH HTTP POST /restconf/config/calls/call/C
  C-SDN ORCH OPS SDN CTRL HTTP POST /restconf/config/calls/call/00009/
  C-SDN ORCH OPS SDN CTRL HTTP POST /restconf/config/calls/call/00010/
  Client      C-SDN ORCH HTTP POST /restconf/config/calls/call/D
  C-SDN ORCH OPS SDN CTRL HTTP PUT /restconf/config/calls/call/00008/
  C-SDN ORCH OPS SDN CTRL HTTP PUT /restconf/config/calls/call/00007/
  C-SDN ORCH OPS SDN CTRL HTTP PUT /restconf/config/calls/call/00009/
  C-SDN ORCH OPS SDN CTRL HTTP PUT /restconf/config/calls/call/00010/
  C-SDN ORCH OPS SDN CTRL HTTP POST /restconf/config/calls/call/00011/
  C-SDN ORCH OPS SDN CTRL HTTP POST /restconf/config/calls/call/00012/
  OPS SDN CTRL C-SDN ORCH WebSocket WebSocket Text [FIN]

OCS
  Client      C-SDN ORCH HTTP PUT /restconf/config/calls/call/00011/
  C-SDN ORCH OPS SDN CTRL HTTP PUT /restconf/config/calls/call/00012/
  C-SDN ORCH OPS SDN CTRL HTTP PUT /restconf/config/calls/call/00009/
  C-SDN ORCH OPS SDN CTRL HTTP PUT /restconf/config/calls/call/00010/
  C-SDN ORCH OPS SDN CTRL HTTP PUT /restconf/config/calls/call/00007/
  C-SDN ORCH OPS SDN CTRL HTTP PUT /restconf/config/calls/call/00008/

```

Fig. 7 Control traffic capture.

set up the DD-OFDM flow (carrying data from OPS domain). The initial occupancy of the OCS domain is shown in Fig. 8a, corresponding to Fig. 4, step I. There it can be observed that the end-to-end 10G-OTN signal (A) was surrounded by the CO-OFDM and DP-QPSK signals (B, C). Both kinds of signals could be successfully received assuming a soft decision forward error correction (FEC) coding. In fact, DP-QPSK signals were featuring BERs below 10^{-5} while CO-OFDM signal was achieving $1.2 \cdot 10^{-2}$ BER. Since OFDM signals had sharp spectral edges (see Fig.8c-d), CO-OFDM and 10G-OTN were narrowly spaced.

Given this initial status, a new request D asked for a

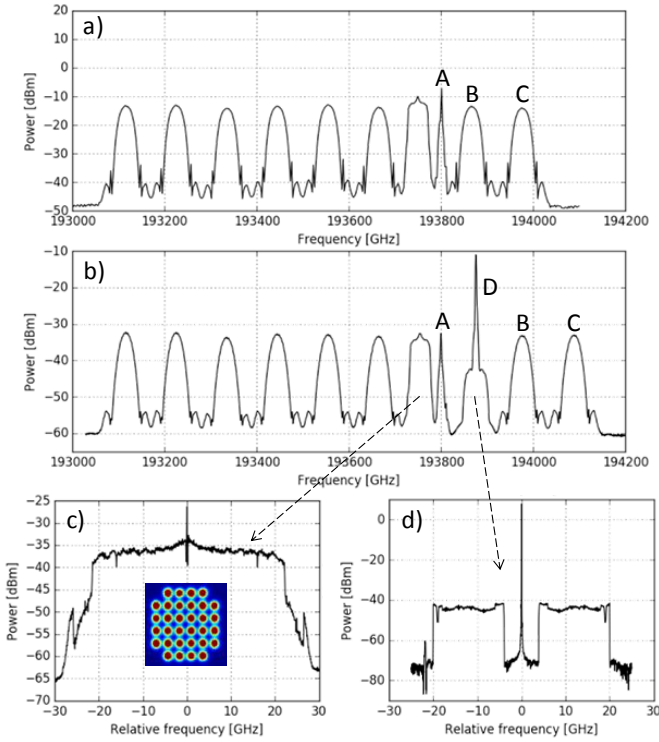


Fig. 8. WDM spectrum before (a) and after (b) adaptive re-allocation. Spectrum of CO-OFDM (c) and DD-OFDM (d) signals.

DD-OFDM flow to be routed through the monitored link. Please note that DD-OFDM is a low-cost solution coping with metro-access distances. In order to further reduce the cost, these transceivers can employ a DFB laser, which have limited tunability, leading to strict bandwidth allocation requirement. Thus, the SDN controller in the OCS domain re-allocated B and C signals, which were occupying the spectrum slot requested for D. Next, D was allocated, 50 GHz-spaced with respect to A, and the performance monitor raised a notification of estimated performance degradation of A (Fig. 7e). In fact, the peak power difference between A and D was 21.6 dB, leading to a possible nonlinear interaction for the spacing initially set. Thus, the SDN orchestrator gradually modified the frequency spacing up to 75 GHz; integrating the new value learnt into the adaptive orchestration. Finally, B and C signals, adjacent to D, were re-allocated according to the new spacing. This is shown in Fig. 8b, corresponding to step V of Fig 4.

Fig. 9 shows the evolution of the estimated signal to noise ratio (SNR) for all subcarriers of the DD-OFDM signal. The different stages of the setup can be identified by colors given in the legend. The best performance is observed for the electrical back-to-back setup. At each step of additional complexity, the SNR drops. The performance of the 50 km optical link is between 12 dB and 22 dB depending on the subcarrier. Eventually, the DD-OFDM channel achieved a total bitrate of 85.6 Gb/s with a BER of $1.3 \cdot 10^{-3}$ (error-free after applying FEC). Consequently, the FEC error-free operation with the required bandwidth in both domains was confirmed for the flow from node C to ROADM 2 (DMT packet to DD-OFDM).

Table I represents the packet loss ratios (PLRs) observed at the IP-based media gate way at the ROADM 2 for the real-time

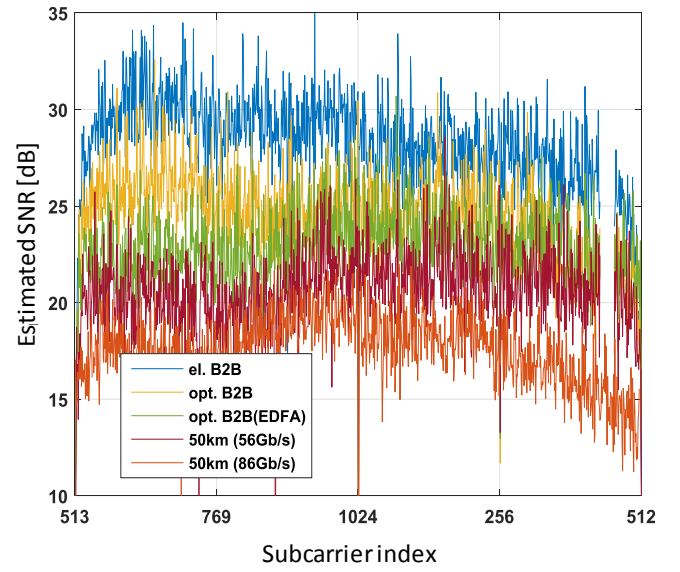


Fig. 9. Per subcarrier SNR for DD-OFDM signal.

| TABLE I PLR OF END-TO-END HD VIDEO STREAMING CHANNEL | |
|---|---------------------------|
| Packet size | 7990 byte (630 ns @ 100G) |
| Average packet rate | 25191 packet/s |
| Effective bit rate | 1.610 Gb/s |
| PLR w/o orchestration | 2.763 % |
| PLR with orchestration | 0.7285 % |

HD video streaming. The initial PLR was 2.76 %, when no adaptive SDN orchestration was performed. Nevertheless, when the aforementioned orchestration was active, the PLR was automatically reduced to 0.728 %.

V. CONCLUSION

Adaptive SDN orchestration of multi-domain multi-technology optical networks has been proposed and experimentally demonstrated. In order to demonstrate the concept, an advanced multi-domain/technology testbed was implemented, consisting on a 400-Gb/s variable-capacity OPS domain and a Tb/s-class flexi-WDM OCS domain. The SDN-controllable transponders and the extended transport API enable the congestion-aware provisioning of end-to-end real-time services. In the control plane, the ABNO architecture has been extended for adaptive SDN orchestration.

A practical use case has been analyzed showing successful end-to-end real-time connectivity across the different domains when enabling the proposed adaptive SDN orchestration. There the key data plane elements were high-capacity programmable S-BVTs and advanced optical performance monitors present at both OCS and OPS network domains.

This constitutes a significant step forward towards, and a cognitive SDN orchestration might be envisioned, as all the key elements are provided. In fact, cognition could be applied in the sense of a feedback control loop, which would process the network monitoring information to validate and provide optimal selection of network resources for satisfying the end-to-end QoS and dynamically re-optimize those service demands. Since the optimization criteria and parameters are all

subject to change dynamically, the potential cognitive SDN orchestrator could re-tune its decisions in order to apply better resource allocation policies.

ACKNOWLEDGMENT

The authors would like to thank Aragon Photonics Labs for providing the high resolution optical spectrum analyzer and Keysight Technologies for providing the arbitrary waveform generator.

REFERENCES

- [1] Y. Yoshida, K.-I. Kitayama, Y. Kai, M. Nishihara, R. Okabe, T. Tanaka, T. Takahara, J. C. Rasmussen, N. Yoshikane, X. Cao, T. Tsuritani, I. Morita, A. Mayoral López de Lerma, J. M. Fabrega, R. Vilalta, R. Casellas, R. Martínez, M. S. Moreolo, R. Muñoz, K. Habel, R. Freund, V. Lopez, A. Aguado, S. Yan, D. Simeonidou, T. Szyrkowiec, A. Autenrieth, M. Shiraiwa, Y. Awaji, N. Wada "First Demonstration of Cognitive SDN Orchestration: A Real-time Congestion-aware Services Provisioning over OFDM-based 400G OPS and Flexi-WDM OCS Networks" In Proc. Optical Fiber Communications Conference 2016, Postdeadline paper Th5B.2.
- [2] Y. Yoshida, A. Maruta, K.-I. Kitayama, M. Nishihara, T. Tanaka, T. Takahara, J. C. Rasmussen, N. Yoshikane, T. Tsuritani, I. Morita, S. Yan, Y. Shu, Y. Yan, R. Nejabati, G. Zervas, D. Simeonidou, R. Vilalta, R. Muñoz, R. Casellas, R. Martínez, A. Aguado, V. López, and J. Marhuenda, "SDN-Based Network Orchestration of Variable-Capacity Optical Packet Switching Network Over Programmable Flexi-Grid Elastic Optical Path Network," in *Journal of Lightwave Technology*, vol. 33, no. 3, pp. 609-617, Feb. 2015.
- [3] A. Rostami, Kun Wang, Z. Ghebretensae, P. Öhlén and B. Skubic, "First Experimental Demonstration of Orchestration of Optical Transport, RAN and Cloud Based on SDN," In Proc. Optical Fiber Communications Conference 2015, Postdeadline paper Th5A.7
- [4] H. Ding, G. Zhang, Y. Li, R. Gong, and Z. Guo, "Experimental Demonstration and Assessment of Multi-Domain SDN Orchestration Based on Northbound API," in Proc. Asia Communications and Photonics Conference 2015, paper ASu4F.1.
- [5] R. Vilalta, V. López, A. Mayoral, N. Yoshikane, M. Ruffini, D. Siracusa, R. Martínez, T. Szyrkowiec, A. Autenrieth, S. Peng, R. Casellas, R. Nejabati, D. Simeonidou, X. Cao, T. Tsuritani, I. Morita, J. P. Fernández-Palacios, R. Muñoz, "The need for a Control Orchestration Protocol in Research Projects on Optical Networking," *Networks and Communications (EuCNC)*, 2015 European Conference on, Paris, 2015, pp. 340-344.
- [6] N. Sambo, P. Castoldi, E. Riccardi, A. D'Erico, A. Pagano, M. Svaluto Moreolo, J. M. Fabrega, D. Rafique, A. Napoli, S. Frigeiro, E. Hugues-Salas, G. Zervas, M. Nölle, J. K. Fischer, A. Lord, J. P. Fernández-Palacios Giménez, "Next Generation Sliceable Bandwidth Variable Transponders," in *IEEE Communications Magazine*, vol. 53, no. 2, pp. 163-171, Feb. 2015.
- [7] M. Svaluto Moreolo, J. M. Fabrega, L. Nadal, F. J. Vilchez, A. Mayoral, R. Vilalta, R. Muñoz, R. Casellas, R. Martínez, M. Nishihara, T. Tanaka, T. Takahara, J. C. Rasmussen, C. Kottke, M. Schlosser, R. Freund, F. Meng, S. Yan, G. Zervas, D. Simeonidou, Y. Yoshida, K. Kitayama, "SDN-enabled Sliceable BVT Based on Multicarrier Technology for Multi-Flow Rate/Distance and Grid Adaptation," in *Journal of Lightwave Technology*, (invited paper), Vol. 34, No. 6, pp. 1516-1522, Mar. 2016.
- [8] A. Aguado, V. López, J. Marhuenda, O. González de Dios, and J. P. Fernández-Palacios, "ABNO: A Feasible SDN Approach for Multivendor IP and Optical Networks [Invited]," in *Journal of Optical Communications and Networking*, vol. 7, no. 2, pp. A356-A362, Feb. 2015.
- [9] JGN-X: <http://www.jgn.nict.go.jp/english/info/index.html>
- [10] H. Harai, H. Furukawa, K. Fujikawa, T. Miyazawa and N. Wada, "Optical Packet and Circuit Integrated Networks and Software Defined Networking Extension," in *Journal of Lightwave Technology*, vol. 32, no. 16, pp. 2751-2759, Aug. 15, 2014.
- [11] J. M. Fabrega, M. Svaluto Moreolo, L. Nadal, F. J. Vilchez, A. Villafranca, and P. Sevillano, "Experimental Study of Adaptive Loading in IM/DD OFDM Using In-band Optical Sub-Carrier SNR Monitoring," in Proc. Optical Fiber Communication Conference, March 2016, paper Th2A.12
- [12] R. Vilalta, A. Mayoral, R. Muñoz, R. Casellas, R. Martínez, "Hierarchical SDN Orchestration for Multi- Technology Multi-Domain Networks with Hierarchical ABNO," In Proc. European Conference on Optical Communication (ECOC 2015), Valencia, Spain, September 2015
- [13] N. Yoshikane, X. Cao, Y. Yoshida, M. Nishihara, M. Shiraiwa, T. Tsuritani, I. Morita, T. Takahara, T. Tanaka, J. C. Rasmussen, N. Wada, K. I. Kitayama, "Demonstration of Dynamic Congestion Control in Optical Packet Switching Network Employing Rate-Adaptive Transmitter and Receiver," in Proc. Photonics in Switching (PS), September 2015